

Quantum entanglement of a large number of photons

H.S. Eisenberg,¹ G. Khoury,¹ G. Durkin,^{1,2} C. Simon,³ and D. Bouwmeester¹

¹*Department of Physics, University of California, Santa Barbara, California 93106, USA*

²*Centre for Quantum Computation, University of Oxford, Oxford OX1 3PU, United Kingdom*

³*Laboratoire de Spectrométrie Physique, CNRS - Université Grenoble I, St. Martin d'Hères, France*

A bipartite multiphoton entangled state is created through stimulated parametric down-conversion of strong laser pulses in a nonlinear crystal. It is shown how detectors that do not resolve photon number can be used to analyze such multiphoton states. Entanglement of up to 12 photons is detected using both the positivity of the partially transposed density matrix and a newly derived criteria. Furthermore, evidence is provided for entanglement of up to 100 photons. The multiparticle quantum state is such that even in the case of an overall photon collection and detection efficiency as low as a few percent, entanglement remains and can be detected.

PACS numbers: 42.65.Lm, 42.50.Dv, 03.65.Ud

In recent years, small numbers of entangled particles have been used for testing quantum mechanics and for implementing various quantum information protocols[1]. However, other tests probing the validity of quantum decoherence models [2], and additional quantum information protocols will require entangled states of large numbers of particles. Bipartite multiphoton states, the subject of this paper, can be used to test foundations of quantum theory[3, 4], and for quantum cryptography[5]. Furthermore, it has been shown that phase sensitive measurements[6] and quantum photolithography[7] can exceed classical boundaries imposed by the wavelength of light, by using multiple entangled photons[8].

In this Letter we demonstrate the generation of a bipartite entangled state of many photons in two spatial modes, as produced by stimulated parametric down-conversion (PDC)[9, 10, 11, 12]. The Hamiltonian for the generation of polarization entangled photons [9] is given by

$$H = i\kappa(a_h^\dagger b_v^\dagger - a_v^\dagger b_h^\dagger) + h.c. \quad (1)$$

Horizontally (h) and vertically (v) polarized photons occupy two spatial modes (a and b); κ is a coupling constant that depends on the nonlinearity of the crystal and the intensity of the pump pulse. The resulting photon state is given by[11]

$$|\psi\rangle = \frac{1}{\cosh^2 \tau} \sum_{n=0}^{\infty} \sqrt{n+1} \tanh^n \tau |\psi_n^-\rangle, \quad (2)$$

$$|\psi_n^-\rangle = \frac{1}{\sqrt{n+1}} \sum_{m=0}^n (-1)^m |n-m\rangle_{a_h} |m\rangle_{a_v} |m\rangle_{b_h} |n-m\rangle_{b_v},$$

where, for example, $|m\rangle_{a_v}$ represents m vertically polarized photons in mode a . The interaction parameter τ depends linearly on the crystal length and on κ . The state $|\psi\rangle$ is a superposition of the states $|\psi_n^-\rangle$ of n indistinguishable photon pairs. Each $|\psi_n^-\rangle$ is an analog of a singlet state of two spin- $n/2$ particles, thus $|\psi\rangle$ is invariant under joint rotations of the polarization bases

of both modes. The average photon pair number is $\langle n \rangle = 2 \sinh^2 \tau$. Although photons are created in pairs, the resulting state cannot be factorized into individual pairs. As a result of the stimulated emission process, the pairs are indistinguishable such that they form a single multiphoton entangled state. Previous PDC experiments have been restricted to $\tau < 0.1$, resulting in the detection of at most 4 to 5 photons in an entangled state[12, 13, 14]. This work addresses the region of $\tau > 1$, where entangled states of large numbers of photons can be generated.

Our setup is switchable between single-pass and double-pass[12] of a pump pulse through a BBO nonlinear crystal (see Fig. 1). The pump is a frequency-doubled amplified Ti:sapphire laser, giving 200 fs pulses with $5 \mu\text{J}$ per pulse. Two down-converted modes a and b are selected by coupling into single-mode fibers through 5 nm narrow bandpass filters, justifying the use of the Hamiltonian of Eq. 1. For each spatial mode, two orthogonal polarizations are separated by a fiber polarization beam splitter and detected by silicon avalanche photodiodes (APD). Single-photon count rates and coincidence rates were recorded as functions of the pump power in three polarization bases: horizontal/vertical linear (hv), plus/minus 45° linear (pm) and right/left circular (rl).

To characterize states of multiple photons, it is desirable to have detectors that can resolve photon number. Although such detectors exist[15, 16, 17, 18, 19], the photon number resolution is always limited by losses. Therefore, to determine the actual multiphoton state produced at the source, it is necessary to perform a probability analysis of the experimental data, based on the physics of the detection scheme.

We use APDs that give no direct information about the number of detected photons. Nevertheless, the probability to obtain a signal depends on the photon number[20, 21]. For a total collection efficiency η (a combination of the APD detectors and the optical coupling efficiencies), the triggering probability given an m -photon

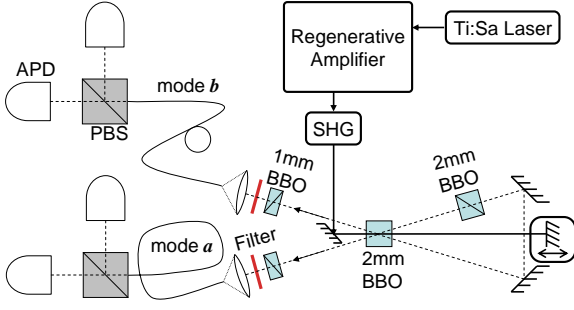


FIG. 1: The experimental setup. The pump pulses pass twice through the nonlinear BBO crystal, with a controlled delay between the passes. Down-converted photons from the first pass are re-injected into the crystal together with the pump second pass[12]. The configuration can be switched to single-pass by blocking the path of the first down-conversion. Additional BBO crystals are inserted in order to compensate for temporal walk-off. The two spatial modes are collected into single-mode fibers through narrow bandpass filters. Photons in the different modes are detected by four APDs.

state is

$$P = 1 - P_0 = 1 - (1 - \eta)^m, \quad (3)$$

where P_0 is the probability of not detecting a photon.

For the state of Eq. 2, the detection probabilities for a single spatial mode and coincidences between any two modes as functions of τ and η were derived. For example, the probability per pulse to trigger a single detector is

$$P = \frac{1}{\cosh^4 \tau} \sum_{n=1}^{\infty} \tanh^{2n} \tau \sum_{m=1}^n (1 - (1 - \eta)^m) \quad (4)$$

$$= \frac{\eta \tanh^2 \tau}{1 - (1 - \eta) \tanh^2 \tau}.$$

We measured probabilities as functions of the pump intensity I up to a maximal intensity I_{max} , and fitted the results with the collection efficiencies η_i of the four modes a_h , a_v , b_h and b_v , and the maximum interaction parameter τ_{max} defined as $\tau_{max} = \tau \sqrt{I_{max}/I}$.

Single-photon counts of one polarization mode and coincidence counts are presented in Fig. 2a. This data is from a single-pass configuration. All the results in various polarization bases were successfully fitted with the same parameters $\tau_{max} = 2.30 \pm 0.05$ and $\eta = 1.9 \pm 0.2\%$ for all four modes, strongly supporting the model of Eq. (1). The stimulated emission enabled the direct observation of coincidences that can only occur from events of at least three or four pairs. By collecting only one polarization and splitting the photons into two detectors with a beam splitter, we counted coincidence events of the form a_h - a_h - b_h and of the form a_h - a_h - b_h - b_h that originated from three (or more) and four (or more) photon-pairs, respectively. Figure 2b combines all the measurements as a function of τ . The larger the number of relevant pairs for an event,

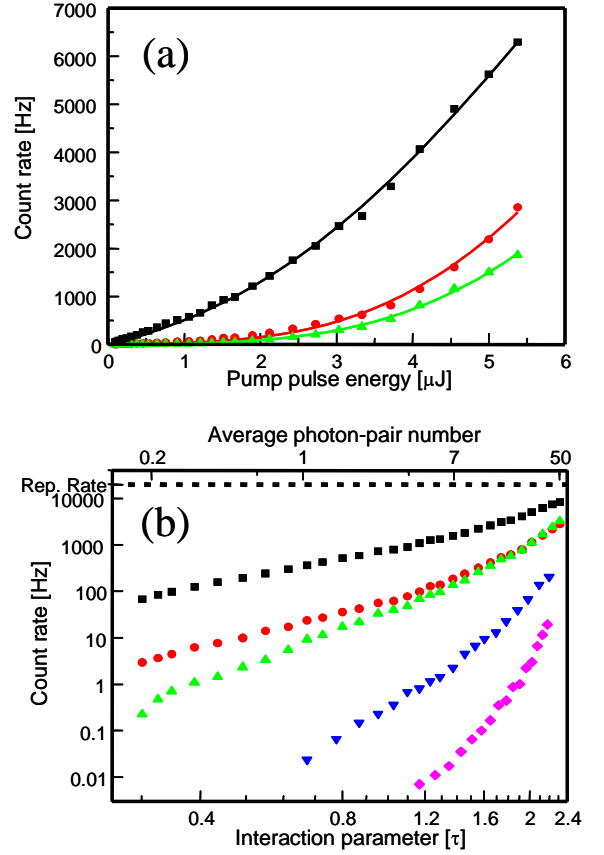


FIG. 2: (a) Experimentally observed single photon count rates of the a_h mode (**squares**), one-pair coincidence rates between a_h and b_v (**circles**) and two-pair coincidence rates between a_h and b_h (**triangles**) as a function of the pump pulse energy. The one-pair coincidences can arise from one or more pairs, while the two-pair coincidences can arise from two or more. Fits are included as solid lines. (b) The τ dependance of the results of Fig. 2a and coincidence events that can be generated by at least three pairs (**inverted triangles**) and four pairs (**diamonds**) of photons.

the steeper is its graph, as expected from a multiphoton stimulated process. The slopes for $\tau < 1$ of the single photon counts and the one-pair coincidence are parallel and linear with pump pulse energy, as both result from one-pair events. All the graphs should saturate for large enough τ at the repetition rate of 20 kHz. The maximum interaction parameter achieved corresponds to 100 photons per pulse on average.

We have shown a stimulated emission process in which many photons are created in a way consistent with the state of Eq. 2. This does not yet prove the specific quantum correlations between the photons described by that state. We will now present two criteria that prove the presence of entanglement. Our approach is to use a low overall detection efficiency such that in the relevant parameter regime we detect at most two photons. We show that entanglement is still present in this situation. This

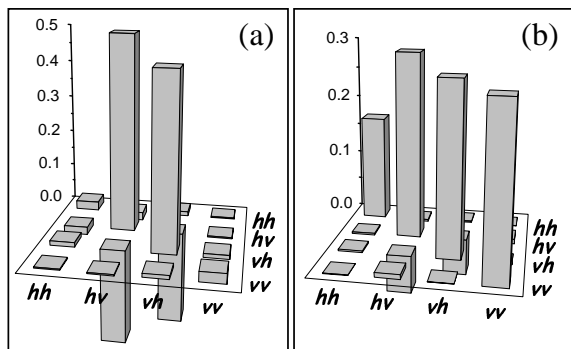


FIG. 3: Measured density matrices in the (1,1) subspace for $\tau = 0.2$ (a) and $\tau = 1.85$ (b). Only the real part of ρ is shown as its imaginary part is negligible.

proves entanglement not only of the detected photons, but also of the initial state before most of the photons were lost, as it is impossible to form an entangled state by applying a local operation to unentangled photons.

The Positivity of the Partially Transposed (PPT) density matrix is a separability (non-entanglement) criterion for bipartite systems, such as the PDC system studied here[22]. Consider the density matrix ρ in the subspace where only one photon after losses is detected in each of the spatial modes. This restriction will be justified below. The total probability for such a detection is $P_{(1,1)} = P_{hv} + P_{vh} + P_{hh} + P_{vv}$, where P_{hv} is the probability to detect a coincidence between a_h and b_v , etc. By only considering events from this (1,1) subspace, probabilities can be normalized as $p_{ij} = P_{ij}/P_{(1,1)}$. We use $|hh\rangle$, $|hv\rangle$, $|vh\rangle$ and $|vv\rangle$ as the basis states for ρ . We also define the single-pair visibility V for different polarization detection bases. For example, in the hv basis for mode a and the pm basis for mode b

$$V_{hv,pm} = \frac{P_{hm} + P_{vp} - P_{hp} - P_{vm}}{P_{hm} + P_{vp} + P_{hp} + P_{vm}}. \quad (5)$$

The elements of ρ can be readily obtained from combinations of visibilities, a process known as state tomography[23]. Density matrices, as measured for low ($\tau = 0.2$) and high ($\tau = 1.85$) values of τ , are presented in Fig. 3. The measured density matrices are consistent with the state of Eq. 2; for low tau the density matrix approaches the familiar two-photon $|\psi_1^-\rangle$ Bell state ($\rho_{hv,hv} = \rho_{vh,vh} = -\rho_{hv,vh} = -\rho_{vh,hv} = 1/2$), for high tau hh and vv coincidences are detected ($\rho_{hh,hh}$ and $\rho_{vv,vv}$ are no longer small) as a result of multiple photon pairs before detection losses. Considering these dominant 6 terms, the partially-transposed matrix ρ^{PT} will only have positive eigenvalues if

$$C_1 = \frac{16 \cdot p_{hh}p_{vv}}{(V_{pm,pm} + V_{rl,rl})^2 + (V_{pm,rl} - V_{rl,pm})^2} > 1. \quad (6)$$

The violation of the above separability criterion proves entanglement. For example, for a pure $|\psi_1^-\rangle$ state C_1 is

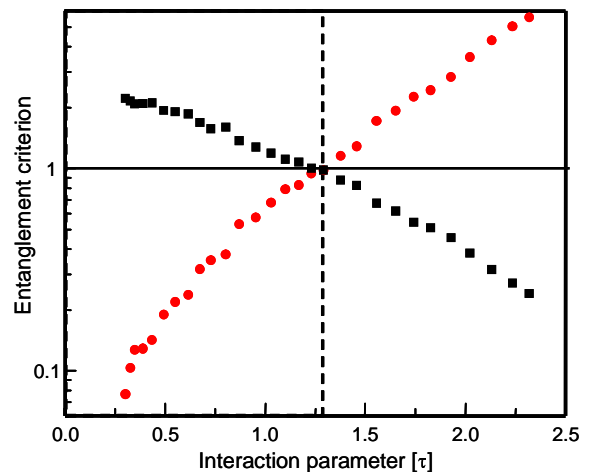


FIG. 4: The experimentally measured entanglement criteria. To detect entanglement the PPT criterion C_1 (circles) must be smaller than one, while the visibility/spin-correlation criterion C_2 (squares) must be larger than one. Both criteria detect entanglement up to an interaction of $\tau = 1.3$ (dashed line), corresponding to a state with 12 photons on average.

zero. The circles in Fig. 4 show the measured C_1 as a function of τ . Entanglement is detected up to an interaction of $\tau = 1.3$, corresponding to 6 indistinguishable photon-pairs on average. For this τ value and detection efficiency of 2%, the ratio of the probabilities for a detection from a higher photon number subspace and from a (1,1) subspace is about 0.06. This low ratio justifies considering only (1,1) subspace events for the density matrix.

We now derive a second separability criterion tailored to detect the type of entanglement created by PDC. The visibility (Eq. 5) can be rewritten as the spin anti-correlation between the two spatial modes[10]:

$$V_{hv,hv} = p_{hv} + p_{vh} - p_{hh} - p_{vv} = -\langle \sigma_z^a \otimes \sigma_z^b \rangle, \quad (7)$$

where σ_i are the Pauli matrices. The total spin correlation is:

$$\begin{aligned} \langle \vec{\sigma}^a \cdot \vec{\sigma}^b \rangle &= \langle \sigma_x^a \otimes \sigma_x^b \rangle + \langle \sigma_y^a \otimes \sigma_y^b \rangle + \langle \sigma_z^a \otimes \sigma_z^b \rangle \\ &= -(V_{pm,pm} + V_{rl,rl} + V_{hv,hv}). \end{aligned} \quad (8)$$

A product state, is maximally correlated (anti-correlated) when the two spins are parallel (anti-parallel). It is convenient to rotate the two correlated spins to one of the principal bases. The correlation in that basis will be ± 1 , and zero in the other two bases. A general separable state (a mixture of product states) can not have a higher correlation. On the other hand, an entangled state such as the Bell $|\psi_1^-\rangle$ state can have all the correlations as -1. Thus, an upper bound criterion for a separable state in the (1,1) subspace is

$$C_2 = |V_{pm,pm} + V_{rl,rl} + V_{hv,hv}| \leq 1. \quad (9)$$

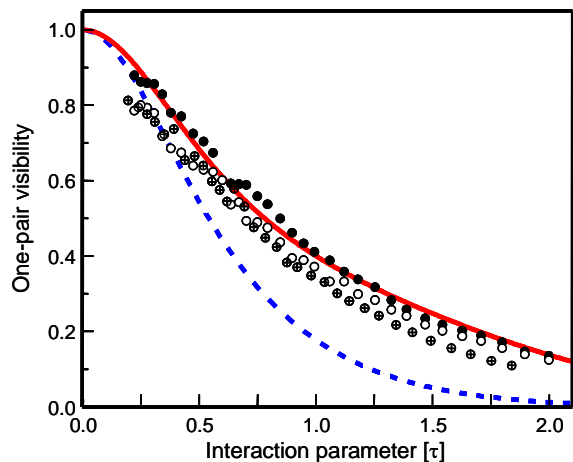


FIG. 5: One-pair visibility as a function of the interaction parameter for the polarization bases hv (solid circles), pm (open circles), and rl (crossed circles), and for the model fit (solid line). The prediction for the ansatz state of distinguishable entangled pairs (dashed line) represents the visibility upper bound for uncorrelated pairs of photons. The observed results are above this bound, indicating the indistinguishable nature of the generated photon-pairs.

The measured values of C_2 are shown as squares in Fig. 4. This second criterion detects entanglement also up to $\tau = 1.3$, or up to about 6 photon pairs. Although based on different arguments, the two criteria detect entanglement up to the same interaction values. This boundary is mainly set by the limitations of the APDs and not by the actual entanglement present in the generated state. One can show theoretically that some entanglement remains for arbitrarily high τ and losses [10, 24].

To provide experimental support for entanglement over the entire detected interaction range, the one-pair visibilities in three polarization bases as measured with a double-pass setup, optimized for collection efficiencies of $\eta = 9 \pm 0.7\%$, are shown in Fig. 5 and compared to their theoretical prediction (solid line). The τ -dependence is approximately the same in the different polarization bases, consistent with the state rotation invariance. For comparison, the visibility for an ansatz state of *distinguishable* pairs of entangled photons was also calculated (see dashed line in Fig. 5). We used the same pair-number distribution as in PDC, but assumed that the different pairs occupy different modes. The predicted visibility for this ansatz state is considerably lower than the PDC visibility curve and the experimental results.

In conclusion we have demonstrated the generation of a bipartite state of up to 50 indistinguishable photon pairs.

Entanglement up to 12 photons has been proven while evidence has been given for entanglement up to 100 photons. We have shown that it is possible to explore quantum entanglement even after the state suffered significant losses and even with detectors that have limited photon number resolution. The studied multiphoton entangled state is of particular interest for quantum cryptography, quantum metrology and for tests of the foundations of quantum mechanics with large-spin systems.

The authors thank M. de Dood and W. Irvine for fruitful discussion. This research has been supported by NSF no 0304678 and DARPA MDA 972-01-1-0027 grants.

-
- [1] D. Bouwmeester, A. Ekert and A. Zeilinger, *The Physics of Quantum Information* (Springer, Berlin, 2000).
 - [2] A. Auffeves *et al.*, Phys. Rev. Lett. **91**, 230405 (2003).
 - [3] P.D. Drummond, Phys. Rev. Lett. **50**, 1407 (1983); N.D. Mermin, Phys. Rev. Lett. **65**, 1838 (1990); A. Peres, Phys. Rev. A **46**, 4413 (1992); W.J. Munro and M.D. Reid, Phys. Rev. A **50**, 3661 (1994).
 - [4] J.C. Howell, A. Lamas-Linares and D. Bouwmeester, Phys. Rev. Lett. **88**, 030401 (2002).
 - [5] G.A. Durkin, C. Simon and D. Bouwmeester, Phys. Rev. Lett. **88**, 187902 (2002).
 - [6] M.J. Holland and K. Burnett, Phys. Rev. Lett. **71**, 1355 (1993).
 - [7] A.N. Boto *et al.*, Phys. Rev. Lett. **85**, 2733 (2000).
 - [8] M.W. Mitchell, J.S. Lundeen, and A.M. Steinberg, Nature **429**, 161 (2004).
 - [9] P.G. Kwiat *et al.*, Phys. Rev. Lett. **75**, 4337 (1995).
 - [10] C. Simon and D. Bouwmeester, Phys. Rev. Lett. **91**, 053601 (2003).
 - [11] P. Kok and S.L. Braunstein, Phys. Rev. A **61**, 042304 (2000).
 - [12] A. Lamas-Linares, J.C. Howell and D. Bouwmeester, Nature **412**, 887 (2001).
 - [13] M. Eibl *et al.*, Phys. Rev. Lett. **90**, 200403 (2003).
 - [14] Z. Zhao *et al.*, Nature **430**, 54 (2004).
 - [15] G.B. Turner *et al.*, SciFi 93 - Conf. on Scintillating Fiber Detectors, 613 (World Scientific, New Jersey, 1993).
 - [16] J.S. Kim *et al.*, Appl. Phys. Lett. **74**, 902 (1999).
 - [17] G. Gol'tsman *et al.*, IEEE Trans. Appl. Superconductivity **11**, 574-577 (2001).
 - [18] E. Waks *et al.*, Phys. Rev. Lett. **92**, 113602 (2004).
 - [19] D. Achilles *et al.*, Opt. Lett. **28** 2387 (2003).
 - [20] D. Mogilevtsev, Opt. Comm. **156** 307 (1998).
 - [21] K.J. Resch, J.S. Lundeen and A.M. Steinberg, Phys. Rev. A **63** 020102(R) (2001).
 - [22] A. Peres, Phys. Rev. Lett. **77**, 1413 (1996).
 - [23] D.F.V. James *et al.*, Phys. Rev. A **64**, 052312 (2001).
 - [24] G.A. Durkin *et al.*, quant-ph/0402053 (2004).